

Three-dimensional data of wirecut surface scans under the confocal microscope (110 character maximum, inc. spaces)

Yuhang Lin^{1,2,*}, Heike Hofmann^{2,3}, Curtis Mosher⁴, Eden Amin⁵, Jeff Salyards², and Alicia Carriquiry^{1,2}

¹Iowa State University, Department of Statistics, Ames, IA, USA

²Iowa State University, Center for Statistics and Applications in Forensic Evidence (CSAFE), Ames, IA, USA

³University of Nebraska-Lincoln, Department of Statistics, Lincoln, NE, USA

⁴Iowa State University, Roy J Carver High Resolution Microscopy Facility (HRMF), Ames, IA, USA

⁵University of Central Oklahoma, Criminal Justice and Forensic Science, Edmond, OK, USA

*corresponding author(s): Yuhang Lin (yhlin@iastate.edu)

ABSTRACT

Update later: max of 170 words: describe the study, the assay(s) performed, resulting data, and reuse potential

Wire cut data is important in forensic investigations but lacks a systematic way of analyzing the data. We created a data set of 120 scans of aluminum wire cut in $x3p$ format, using 5 wire cutters and 3 locations along the 4 blades, with 2 replicates for each combination. A systematic pipeline with multiple analysis plots was developed to analyze the data and draw conclusions based on numerical measures.

Background & Summary

Wire cut data is a type of forensic tool mark data used to identify the source of a wire cutter based on the striations left on the surface. There have been cases where the evidence and testimony on wire cut evidence played a crucial role in the criminal investigation and conviction of a defendant.

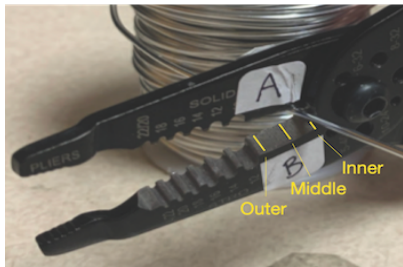
However, there is a lack of a standardized method to analyze it except for visual comparison. Although the Association of Firearm and Toolmark Examiners (AFTE) developed the Theory of Identification¹, which outlines the process of comparing tool marks, it is still subjective and relies on the examiner's experience, making results hard to reproduce and validate. Several reports, such as those from the National Research Council² and the President's Council of Advisors on Science and Technology³, pointed out the abovementioned issues and called for more objective and reproducible methods to analyze tool marks. Early research by Ma et al.⁴ and Zheng et al.⁵ has focused on collecting and distributing datasets for this purpose and providing a foundation for future advancements in tool mark analysis. Studies such as those by Chu et al.⁶ and Vorburger et al.⁷ have demonstrated the efficacy of using numerical methods to improve accuracy and consistency in tool mark analysis. Hare et al.⁸ and Ju et al.⁹ have explored methods for quantifying the similarity between representative signals, but alignment remains a major hurdle.

In this study, we would like to follow the same path and provide a data set of wire cut scans, and also discuss a systematic pipeline to analyze the data and draw conclusions based on numerical measures. Here, we provide a data set containing multiple files, as described in Table 1.

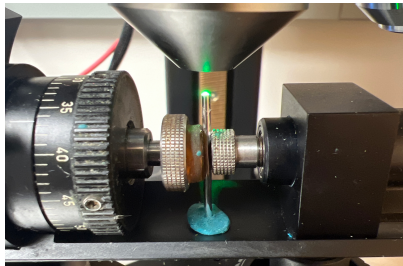
For the reproducibility of all our data and alignment results, we introduce in detail in [Cutting Wires](#) how we cut the wire and collect the 120 scans with 5 tools on 3 locations, in [Extract Profiles](#) how we extract profiles from the scans, in [Filtered Signals](#) how we filter signals from the profiles, in [Align Signals](#) how we align signals from different scans and optimize the alignment with the cross-correlation function (CCF) values. In [Data Records](#), we discuss where our data is held. Then, in [Technical Validation](#), a technical validation was conducted to further compare signals from different sources also match our assumption, together with visual aids for drawing conclusions. Finally, in [Usage Notes](#), we provide available codes for creating the data set and conducting technical validation, as discussed in [Methods](#) and [Technical Validation](#). [Code availability](#) discusses where these codes can be found online. We hope this pipeline developed using this data set can be further generalized and applied to real crime scenes to help investigators draw conclusions based on real wire cut data.

Table 1. Structure of available data and files.

	Description	Section
Raw data		
scans /	folder containing 120 topographic 3d scans of aluminum wire cuts in x3p format	Cutting Wires
meta.csv	meta information for each cut with tool, blade, and location information (csv format)	Cutting Wires
Manual derivatives		
profiles	folder of files with manually extracted profiles (csv format)	Extract Profiles
Computational derivatives		
signals	folder of signals, processed from corresponding profile (csv format)	Filtered Signals
CCF values	CCF values of all pairwise aligned signals in 1 CSV	Align Signals
Image files		
aligned-signals	pictures of pairwise aligned signals from same sources in PNGs	Align Signals



(a)

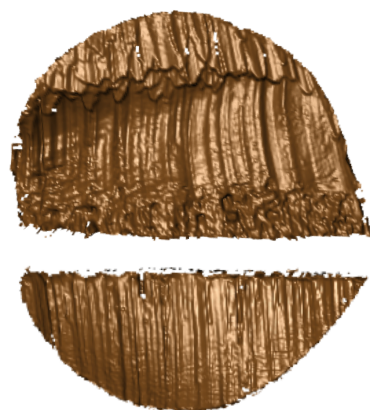


(b)

Blade A



Blade C



Blade B

(c)

Blade D

Figure 1. (a) A Kaiweets wire cutter of model KWS-105 was used to cut the wire, with inner, middle and outer locations marked. (b) A confocal microscope was used to scan the wire surfaces. (c) After separating 2 tent structures by the connecting position, we obtained 4 samples - 2 samples from blade A and B, and others from blade C and D. width and height are tuned manually | full requirements see <https://www.nature.com/sdata/publish/submission-guidelines#figures>

41 Methods

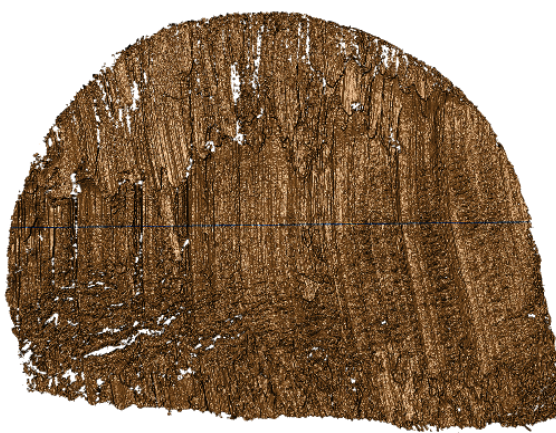
42 In this study, aluminum wire was used to create an optimal scenario where the most amount of information could be transferred
 43 from the tool to the substrate, despite the wire in some real cases being made of lead. The physical property of aluminium
 44 wire make it an excellent candidate for keeping marks while being relatively easy to bend and non-toxic.

45 Cutting Wires

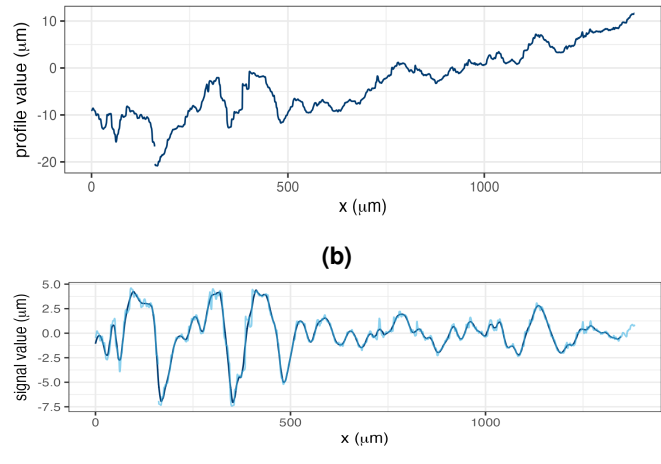
46 The aluminum wire used was 16 Gauge/1.5 mm, anodized. In order to cut the wire, 4-inch pieces were unspooled and cut using
 47 Kaiweets wire cutters, model KWS-105, as shown in Figure 1a, for 1 blade location, either inner, middle, or outer, which gives
 48 us 1 replicate. Each piece was then cut into half to create 2-inch pieces for each side, AB and CD, with a sharpie line marking
 49 the cut ends, giving us 4 samples. Then, we can use the standard scanning protocols for the confocal microscope, shown in
 50 Figure Figure 1b, to scan the wire tip surfaces. The scanned surfaces are saved in a resolution of $0.645\mu\text{m} \times 0.645\mu\text{m}$ per
 51 square pixel in an x3p file format. Here, we are showing AB and CD sides in Figure 1c, with the back of A being C and the
 52 back of B being D. Both AB and CD sides form tent structures on the tips of the wire, and we can separate each side of the
 53 tent into 2 pieces along the bending position, resulting in 8 scans. We repeated this process for all 3 locations along the blade
 54 and 5 wire cutters, with 2 replicates for each tool-edge-location combination, resulting in 120 scans. Each piece was labeled
 55 with the naming conventions, T(ool) 1/2/3/4/5 (Edge) A/B/C/D W(ire) - L(ocation) I(nner)/M(iddle)/O(uter) - R(epetition)
 56 1/2, with T1AW-LI-R1 being the piece cut by tool 1 on the A edge at the inner location for the first repetition.

57 Extract Profiles

58 Numerical comparisons between 2 replicates cannot be done directly on the x3p files. We need to extract representative
 59 functions from the scans first. A representative function with the most information is considered as a signal for one scan,
 60 which can be used for comparison later. To obtain this function, we first need a profile of the scan, which is a sequence of
 61 values along a user-drawn line on the surface. The profile should capture most features of the scan, and be orthogonal to the
 62 striation marks of the scan, which are formed by ups and downs of grooves. So, we draw the line across the wide region of
 63 the scan to maximize the feature captured, as shown in dark blue in Figure 2a. We can then investigate the values under this
 64 profile line. The profile function is along the line is plotted in Figure 2b.



(a)



(b)

(c)

Figure 2. (a) A profile line in dark blue was drawn across the striations of the scan. (b) The profile function extracted along the profile line in (a). (c) The raw signal in light blue is obtained by using the low-pass filter on the profile function in (b) and the filtered signal is obtained by using the high-pass filter on the raw signal.

65 Filtered Signals

66 With the profile extracted, we can then obtain the signal. Two Gaussian filters as discussed in Cleveland et al.¹⁰ are applied
 67 to these resulting profiles. In particular, we first used a large low-pass filter with bandwidths of 400 microns to remove large
 68 trend, as it can overwhelm the signals, and then used a small high-pass filter of 40 microns to average across noise and remove
 69 spikes, as shown in Figure 2c. (add reference: W. S. Cleveland, E. Grosse and W. M. Shyu (1992) Local regression models.
 70 Chapter 8 of Statistical Models in S eds J.M. Chambers and T.J. Hastie, Wadsworth & Brooks/Cole.). Finally, the extreme tail
 71 values are removed.

72 Align Signals

73 Signals extracted from different scans can be put together for comparison, and we maximize the cross-correlation function
 74 (CCF) values between the signals to numerically find the best alignment. For example, we compare T1AW-LI-R1 to T1AW-
 75 LI-R2, T1CW-LI-R1 to T1CW-LI-R2, and so on. That is comparing each row in Figure 3. We know that signals from two
 76 replicates with the same tool-edge-location combination should yield similar signals as in the first and second column of
 77 Figure 4, which will give alignments of massive overlapping and high CCF values close to 1. The alignments and values we
 78 got in the rightmost column of Figure 4 fulfill our expectations.

79 Data Records

80 The complete data set is available on the ISU DataShare repository at <https://iastate.figshare.com/>, which is public and open
 81 access for every interested researcher. The structure of the data set is described before in Table 1.

82 Technical Validation

83 For the data collection process, two team members did the cutting and labeling together, then one person did the scanning and
 84 named according to the naming convention above. The scanning was done in a specific order to ensure consistency across all
 85 scans. The data was saved in a consistent format to ensure they could be easily accessed and analyzed. A third person then
 86 checked the data to ensure that the data was consistent in naming and accurate.

87 For the validation of the scans and their processing we investigate the correlation scores of pair-wise aligned signals. Large
 88 scores between signals are indicative of being made by the same tool. As showed previously in Figure 4 in Align Signals, we
 89 would expect a high correlation score between signals from scans of wires cut with the same tool. For signals from scans of
 90 wires cut with a different tool, we would expect a low correlation score. For example, we have two scans from different tools,
 91 T1AW-LI-R1 and T2AW-LI-R1, as shown in Figure 5a and Figure 5b. The alignment is shown in Figure 5c with 0.2 CCF
 92 value, which is low, as expected.

Table 2. Overview of available codes.

	Description	Section
Inspect raw scans		
1-create_pngs_from_x3p.R	obtain images of x3ps in scans/	Cutting Wires
Extract profiles		
2-create_profiles_from_x3p.R	manually extract profiles from each scan	Extract Profiles
3-create-single-profile-file.R	create meta profile information	Extract Profiles
Derive signals		
4-create_signals_from_profiles.R	derive signals from each profile	Filtered Signals
Align signals		
5-create-images.R	create images for pairwise alignment	Align Signals
6-align-pairwise.R	compute pairwise alignment CCF values	Align Signals
7-all-comparison-results.R	visualize comparison results	Align Signals

93 We also put resulting CCFs for all pairwise comparisons in the boxplot, together with the receiver operating characteristic
94 (ROC) curve, as in Figure 6 and Figure 7. We can see that the CCF values for the same sources are close to 1, while the CCF
95 values for different sources are much lower than expected. This is consistent with our expectations and validates our data
96 processing pipeline.

97 Usage Notes

98 The R package `x3ptools`¹¹ available from CRAN supports working with files in x3p format. The sample scripts in
99 R for processing scans from x3p format to their signal and alignment are available on GitHub `heike/wirecuts-data` in
100 assessment/code folder, as described in Table 2.

101 We already conduct pairwise comparisons and visualize some of the comparison results in Align Signals and Technical
102 Validation, and we can also produce other analysis plots.

103 Suppose we put the CCF values in a tilemap with different tool, location and edge combinations. In that case, we expect
104 only the diagonal to have high CCF values, close to 1 and marked as orange in the tilemap, as the diagonal represents the
105 same source, and the rest of the matrix to have low CCF values, close to 0 and marked as gray. In Figure 8, the behavior is
106 consistent with our expectation overall, except for some rare cases with tool 5 edge D. The density plot in Figure 9 shows the
107 distribution of the CCF values with the same sources and different sources. The overlapping points between the tails of these
108 two distributions can be a rough threshold.

109 Furthermore, the ROC curve in Figure 7 shows the sensitivity / true positive rate against the false positive rate (FPR) (1 -
110 specificity). The curve is very close to the upper left corner, which is excellent for classification and drawing conclusion. It
111 gives us a true threshold of 0.589 to control the FPR to be less than 0.05 with false negative rate (FNR) to be 0, (false positive
112 rate (FPR) / false discovery rate (FDR) -> define the H0 or call it false identification rate (FIR)???, and 0.658 to control the
113 FPR to be less than 0.01, with FNR to be 0.02.

114 **Code availability**

115 We made available all codes we used for inspecting raw scans, extracting profiles, deriving signals, aligning signals, and visual-
116 izing comparison results discussed in [Methods](#) and [Technical Validation](#), as described in Table 2. All results are reproducible
117 using these codes provided.

118 **References**

- 119 1. AFTE. The association of firearm and tool mark examiners: Theory of identification as it relates to toolmarks. *AFTE J.*
120 **30**, 86–88 (1998).
- 121 2. NRC. *National Research Council: Strengthening Forensic Science in the United States: A Path Forward* (National
122 Academies Press, 2009).
- 123 3. President's Council of Advisors on Science and Technology. *President's Council of Advisors on Science and Technology: Forensic Science in Criminal Courts: Ensuring Scientific Validity of Feature-Comparison Methods* (Executive Office of
124 the President of the United States, President's Council, Washington, D.C., 2016).
- 125 4. Ma, L. *et al.* NIST Bullet Signature Measurement System for RM (Reference Material) 8240 Standard Bullets. *J. Forensic
126 Sci.* **49**, 1–11, [10.1520/JFS2003384](https://doi.org/10.1520/JFS2003384) (2004).
- 127 5. Zheng, X. A., Soons, J. A. & Thompson, R. M. NIST Ballistics Toolmark Research Database | NIST (2016).
- 128 6. Chu, W., Thompson, R. M., Song, J. & Vorburger, T. V. Automatic identification of bullet signatures based on consecutive
129 matching striae (CMS) criteria. *Forensic Sci. Int.* **231**, 137–141, [10/gn65cz](https://doi.org/10/gn65cz) (2013).
- 130 7. Vorburger, T. *et al.* Applications of cross-correlation functions. *Wear* **271**, 529–533, [10.1016/j.wear.2010.03.030](https://doi.org/10.1016/j.wear.2010.03.030) (2011).
- 131 8. Hare, E., Hofmann, H., Carriquiry, A. *et al.* Automatic matching of bullet land impressions. *The Annals Appl. Stat.* **11**,
132 2332–2356, [10.1214/17-AOAS1080](https://doi.org/10.1214/17-AOAS1080) (2017).
- 133 9. Ju, W. & Hofmann, H. The R Journal: An Open-Source Implementation of the CMPS Algorithm for Assessing Similarity
134 of Bullets. *The R J.* **14**, 267–285, [10.32614/RJ-2022-035](https://doi.org/10.32614/RJ-2022-035) (2022).
- 135 10. Cleveland, W. S., Grosse, E. & Shyu, W. M. Local Regression Models. In *Statistical Models in S* (Routledge, 1992).
- 136 11. Hofmann, H., Vanderplas, S., Krishnan, G. & Hare, E. X3ptools: Tools for Working with 3D Surface Measurements,
137 [10.32614/CRA.N.package.x3ptools](https://doi.org/10.32614/CRA.N.package.x3ptools) (2018).
- 138

139 **Acknowledgements**

140 This work was partially funded by the Center for Statistics and Applications in Forensic Evidence (CSAFE) through Cooperative
141 Agreement 70NANB20H019 between NIST and Iowa State University, which includes activities carried out at Carnegie
142 Mellon University, Duke University, University of California Irvine, University of Virginia, West Virginia University, University
143 of Pennsylvania, Swarthmore College and the University of Nebraska-Lincoln.

144 **Author contributions statement**

145 Let's follow the Elsevier definitions: <https://www.elsevier.com/researcher/author/policies-and-guidelines/credit-author-statement>
146 Y.L.: Methodology, Software, Validation, Data Curation, Writing - Draft; H.H.: Conceptualization, Methodology, Validation,
147 Writing - Review & Editing; C.M.: Lab supervision; E.A.: Physical Specimen, Scanning; J.S: Forensic advice; A.C.:
148 Funding acquisition.
149 All authors reviewed the manuscript.

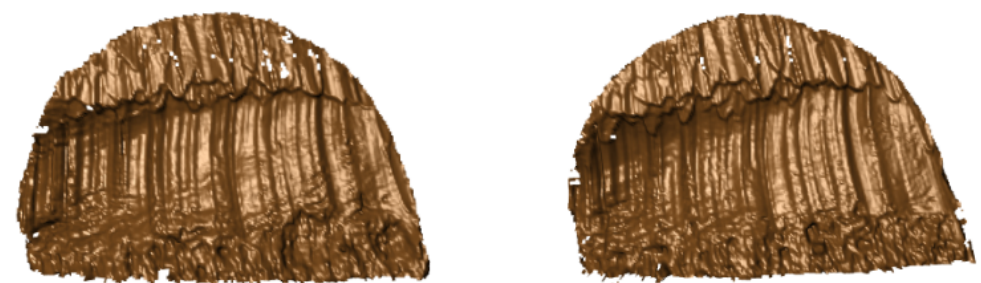
150 **Competing interests**

151 (mandatory statement)
152 H.H. is a technical advisor to AFTE (Association of Firearms and Toolmarks Examiners), fellow of the ASA (American
153 Statistical Association), and committee member of the ASA Forensic Science Committee. H.H. has testified as court witness
154 on behalf of judge April Neubauer, NY State Supreme Court Criminal Term in New York City. [other competing interests -](#)
155 [Alicia?](#)

Edge A



Edge C



Edge B



Edge D



Figure 3. Scans from different sides of tool 1 at the inner location.

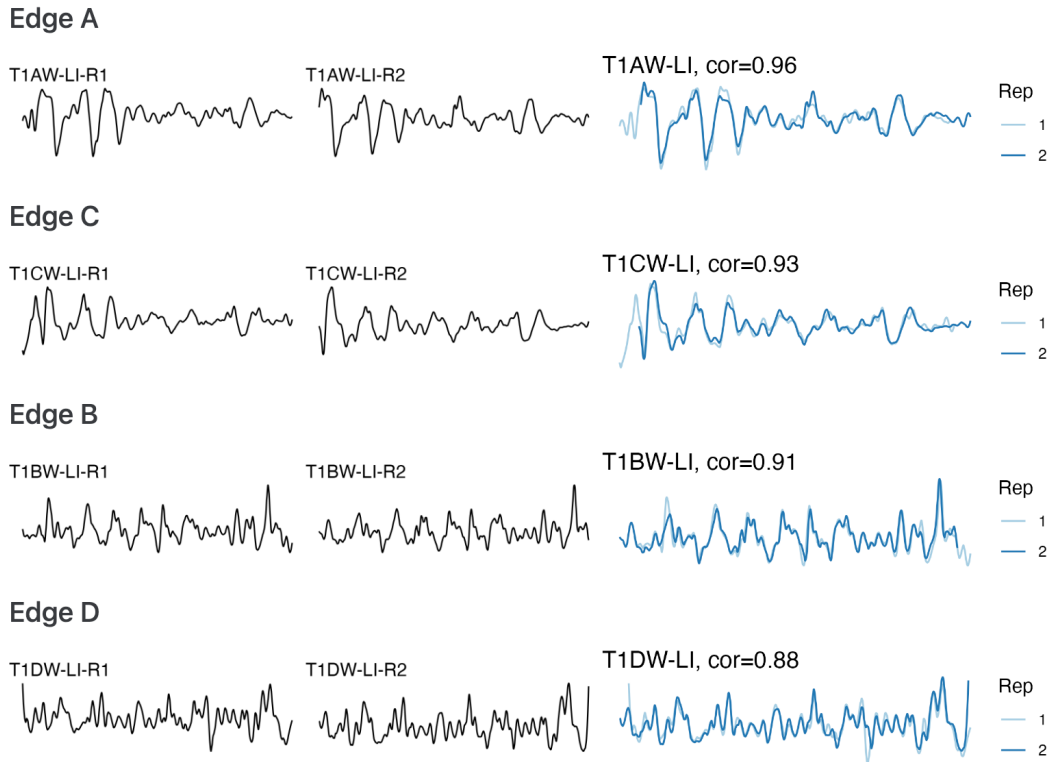


Figure 4. The first and second columns show the signals extracted from Figure 3, and the third column shows the alignments and CCF values between pairs of signals.

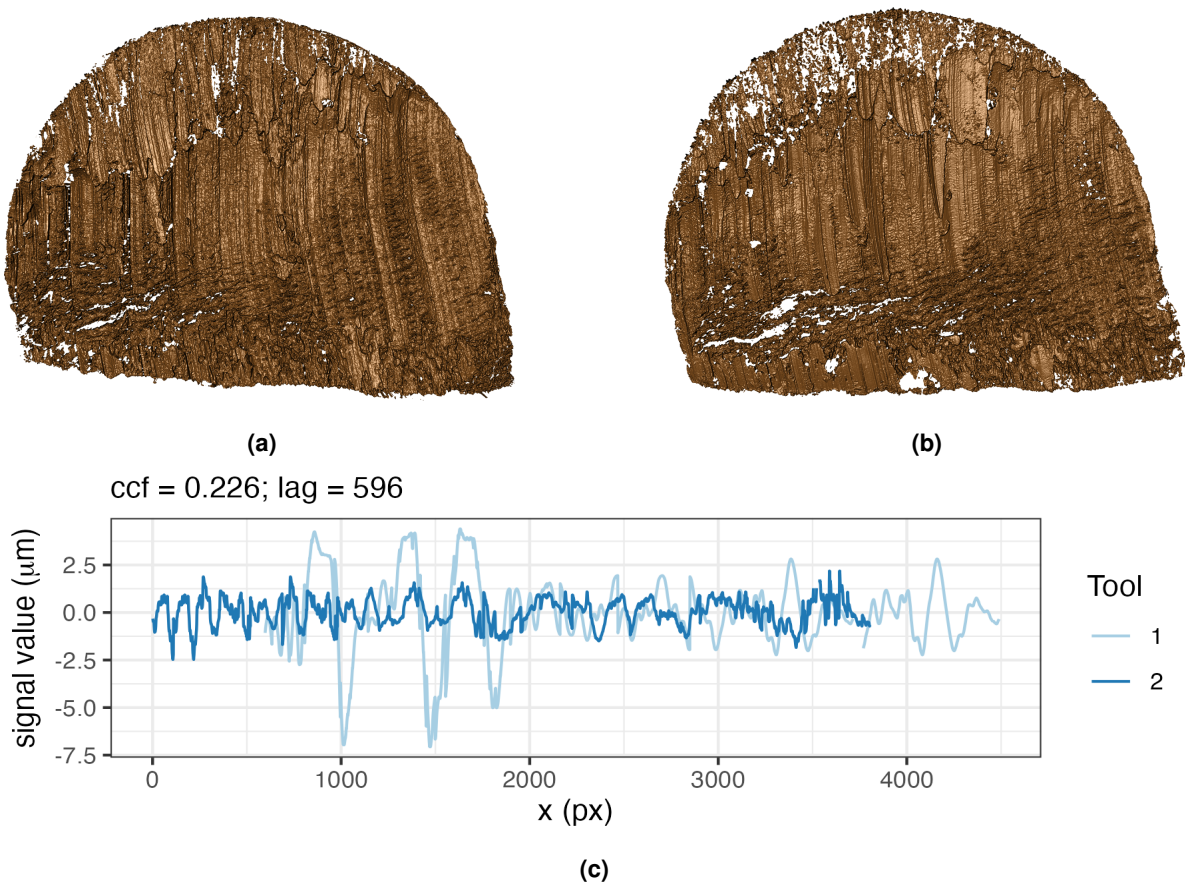


Figure 5. (a) Scan T1AW-LI-R1 cut by tool 1. (b) Scan T2AW-LI-R1 cut by tool 2. (c) Alignment of signals from T1AW-LI-R1 and T2AW-LI-R1.

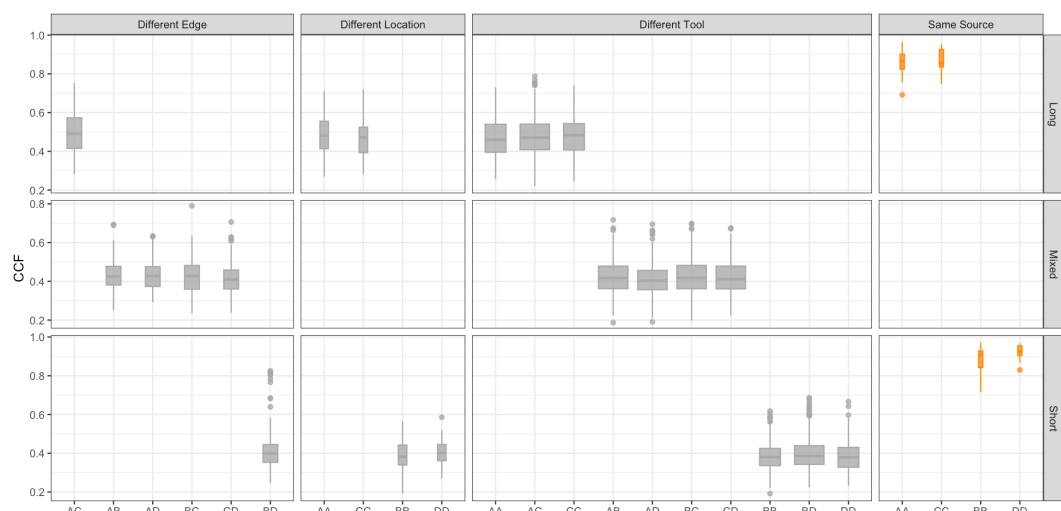


Figure 6. The boxplot shows that signals from the same sources have higher CCFs than those from different sources.

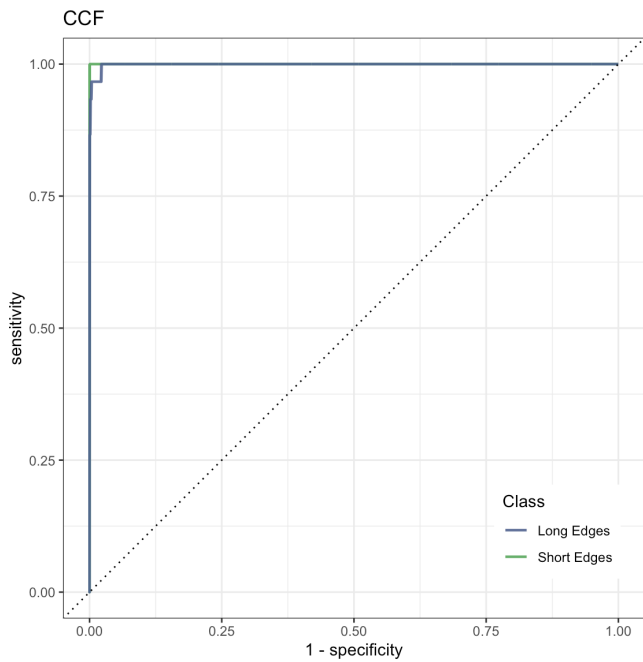


Figure 7. The ROC curve is bending very close to the upper left corner, which means excellent in classification and drawing conclusions.

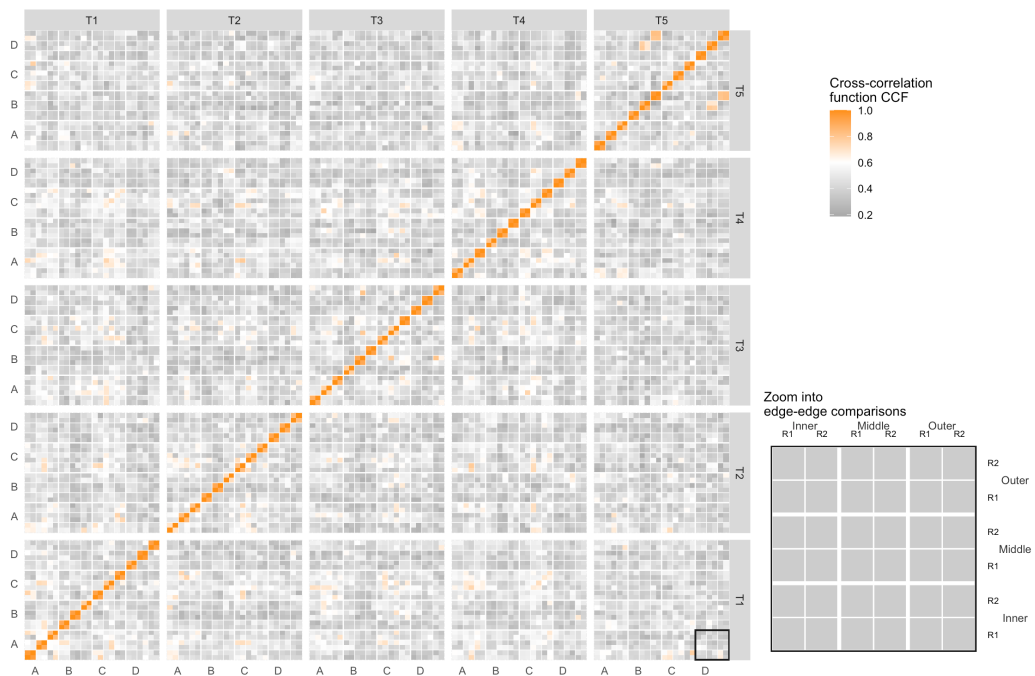


Figure 8. The tilemap shows signals from the same source have CCFs close to 1.

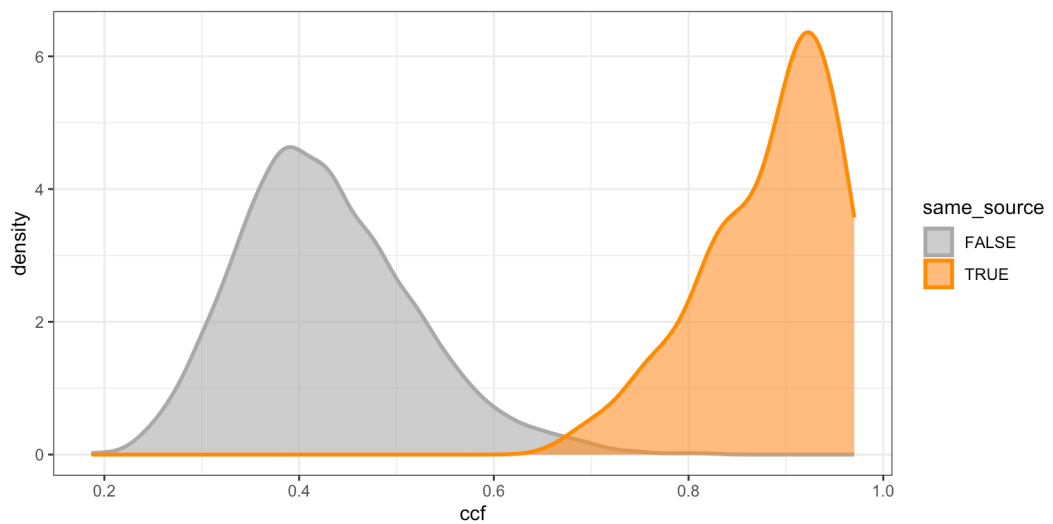


Figure 9. The density plot shows tails of distributions overlap, which can be used as a rough threshold for drawing conclusions.